IOP Publishing New J. Phys. 26 (2024) 013053 https://doi.org/10.1088/1367-2630/ad1a27

New Journal of Physics
The open access journal at the forefront of physics

Deutsche Physikalische Gesellschaft DPG
IOP Institute of Physics

Published in partnership with: Deutsche Physikalische Gesellschaft and the Institute of Physics

OPEN ACCESS

RECEIVED
27 March 2023

REVISED
19 December 2023

ACCEPTED FOR PUBLICATION
3 January 2024

PUBLISHED
30 January 2024

PAPER

Measuring relational information between quantum states, and applications

Michał Oszmaniec[1,2,*], **Daniel J Brod**[3] **and Ernesto F Galvão**[3,4]

[1] Center for Theoretical Physics, Polish Academy of Sciences, Al. Lotników 32/46, 02-668 Warsaw, Poland
[2] NASK National Research Institute, Kolska 12, Warsaw 01-045, Poland
[3] Instituto de Física, Universidade Federal Fluminense, Niterói, RJ 24210-340, Brazil
[4] International Iberian Nanotechnology Laboratory (INL), Av. Mestre Jose Veiga, 4715-330 Braga, Portugal
[*] Author to whom any correspondence should be addressed.

E-mail: oszmaniec@cft.edu.pl

Keywords: relational information, unitary invariance, Bargmann invariants, nonclassicality, measurement protocol

Supplementary material for this article is available online

Abstract

The geometrical arrangement of a set of quantum states can be completely characterized using relational information only. This information is encoded in the pairwise state overlaps, as well as in Bargmann invariants of higher degree written as traces of products of density matrices. We describe how to measure Bargmann invariants using suitable generalizations of the SWAP test. This allows for a complete and robust characterization of the projective-unitary invariant properties of any set of pure or mixed states. As applications, we describe basis-independent tests for linear independence, coherence, and imaginarity. We also show that Bargmann invariants can be used to characterize multi-photon indistinguishability.

1. Introduction

The relative geometrical arrangement of a set of quantum states determines properties such as the Hilbert space dimension they span, or whether they can be simultaneously diagonalized. These properties are physically meaningful, being independent of gauge choices for the global phase of each state's wave-function, and invariant under application of the same unitary transformation on all quantum states in the set. More generally, we use the terms *relational* or *Projective-Unitary* (PU) invariants to refer to properties of tuples of quantum states that are invariant under application of the same unitary transformation to each state in the tuple. The simplest example of a relational invariant is the two-state overlap $\Delta_{12} = \mathrm{tr}(\rho_1\rho_2)$, which for pure states reduces to $\Delta_{12} = |\langle\psi_1|\psi_2\rangle|^2$, with a clear operational physical interpretation.

One way to fully characterize relational information in a tuple of (generally mixed) quantum states, $\mathcal{S} = (\rho_i)_{i=1}^N$, is to perform individual tomographic reconstruction of each state. This is both experimentally costly and unnecessary, providing much more information than strictly needed. A more economical approach is to directly measure a set of invariant properties of a tuple of quantum states. We call such a set *complete* if it allows us to decide whether two tuples of quantum states $\mathcal{S} = (\rho_i)_{i=1}^N, \mathcal{S}' = (\sigma_i)_{i=1}^N$ are unitarily equivalent, in the sense that there exists a unitary operator U taking states from $\mathcal{S}$ onto their counterparts in $\mathcal{S}'$: $\sigma_i = U\rho_i U^\dagger$. In the above, we identified the relational properties of quantum states with equivalence classes (orbits) of the unitary group acting on tuples of quantum states. This approach follows the spirit of the Erlangen program in Geometry [1] (i.e. studying geometry via the lens of group actions and their invariants) and is justified by the fact that unitary channels constitute the most general invertible operations allowed in quantum theory. Note that the same paradigm motivated the usage of invariant polynomials in the context of classification of entanglement classes subject to local unitary transformations [2].

Here we introduce quantum circuits we call *cycle tests*, which enable the direct measurement of complete sets of Bargmann invariants for both mixed and pure quantum states. We review previous mathematical literature identifying complete sets of invariants for different scenarios. For the case of pure states, we show all necessary invariants can be incorporated in a single Gram matrix $G_{ij} = \langle\psi_i|\psi_j\rangle$, with suitable gauge

choices so that all parameters in G are PU-invariants measurable by our proposed circuits. This operational approach to measuring and using Bargmann invariants results in applications such as multi-photon indistinguishability certification, and basis-independent tests of linear independence, imaginarity, and coherence.

We start by reviewing the definition of Bargmann invariants. Consider a tuple of m pure quantum states (understood as rank one normalized projectors) $\Psi = (\psi_1, \psi_2, \ldots \psi_m)$, where we used the shorthand $\psi_j = |\psi_j\rangle\langle\psi_j|$. We later consider the generalization to mixed states. The Bargmann invariant of this tuple of states is defined as [3, 4]:

$$\Delta_{12\cdots m} = \langle\psi_1|\psi_2\rangle\langle\psi_2|\psi_3\rangle\cdots\langle\psi_m|\psi_1\rangle\,. \tag{1}$$

We say that this invariant has *degree m*. Due to the suitable arrangement of bras and kets, the above expression is a well-defined PU-invariant function of states in Ψ. Note that, for $m = 2$, this invariant reduces to the overlap $\Delta_{12} = |\langle\psi_1|\psi_2\rangle|^2$. Bargmann invariants have been studied in the context of characterization of photonic indistinguishability [5–7] and geometric phases [8, 9]. The Kirkwood–Dirac quasi-probability representation [10–12] is also defined in terms of these invariants. The phase of $\Delta_{12\cdots m}$ is precisely the Pancharatnam geometric phase [13] acquired by a wavefunction $|\psi_1\rangle$ subjected to a sequence of projective measurements onto states $\psi_m, \ldots, \psi_2, \psi_1$. Equivalently, it is the Berry phase acquired by a cyclic trajectory along the shortest (geodesic) cyclic path visiting those states [14]—for a review of these ideas, see [9]. Bargmann invariants are also known as multivariate traces [15], and have been studied in mathematical invariant theory [16]. Some of the more recent applications involve the description of error mitigation techniques [17], scalar spin chirality [18], weak values [19], and out-of-time-ordered correlators [20].

2. Results

2.1. Measuring Bargmann invariants

Let us now describe a quantum circuit family that measures any Bargmann invariant $\Delta_{12\cdots m}$. We call these circuits *cycle tests*, and they are generalizations of the well-known SWAP test [21, 22] used to measure the two-state overlap Δ_{12} (see figure 1(a). The key gate in the cycle test circuit of figure 1(b) is a controlled cycle permutation, which implements the cyclic permutation $(12\cdots m)$ of the input states when the control qubit is in state $|1\rangle$, and identity otherwise. It is easy to check that the final measurement of the auxiliary qubit gives an estimate of $\Re(\Delta_{12\cdots m})$. The circuit of figure 1(b) was proposed in [23] as a way to measure non-linear functionals of a single density matrix. Here, we use it with different inputs to estimate $\Re(\Delta_{12\cdots m})$, and propose a modification with an added phase gate $P = \mathrm{diag}(1, i)$, to enable the measurement of $\Im(\Delta_{12\cdots m})$ (see figure 1(b). Note that the cycle test reduces to the SWAP test for $m = 2$ states. Overlaps can also be evaluated as a particular case of degree-3 invariants, as $\Delta_{iij} = \Delta_{ij} = |\langle\psi_i|\psi_j\rangle|^2$ — lower-degree invariants can always be recovered from higher-degree invariants with repeated indices. The cycle test circuit can be implemented in linear depth using nearest-neighbor gates only, or in a depth that scales like $O(\log m)$ if we assume all-to-all qubit connectivity, as we describe in the Methods section. After completion of our work, circuits were proposed to measure Bargmann invariants in constant depth [15], or exploring trade-offs between number of auxiliary qubits and depth [17].

An early proposal of a circuit similar to the SWAP and cycle tests in figure 1 appeared in the DQC1 model of quantum computation [24], but using a generic controlled unitary, and an input of maximally mixed states. Circuits of the form of figure 1(b) but with a generic controlled unitary U are often called Hadamard tests [25]—our cycle test circuit can be understood as a Hadamard test of the cyclic permutation operator, featuring a generic product state input.

2.2. Complete characterization of relational information between states

The following Theorem gives a complete characterization of PU-invariant properties of a collection of N pure sates in terms of Bargmann invariants.

Theorem 1 (Characterization of relational properties of pure states). *Let $\Psi = (\psi_i)_{i=1}^N$ be a tuple of pure quantum states. Then, the PU-equivalence class of Ψ is uniquely specified by values of at most $(N-1)^2$ Bargmann invariants. The invariants are of degree $m \leqslant N$ and their choice depends on Ψ.*

The above Theorem follows from results obtained by Chien and Waldron in [4]. In what follows we present a simplified and shortened proof. Our strategy is based on encoding complete PU-invariants in a single Gram matrix in a way that depends on orthogonality relations of states in Ψ. This allows us to upper bound the number of necessary invariants by $(N-1)^2$. An early result along these lines was obtained in [26], which proposes an explicit canonical form for the Gram matrix for the case of no null overlaps.

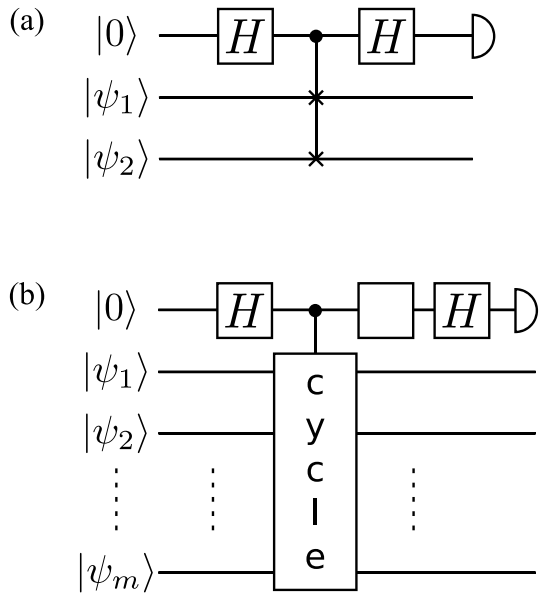

Figure 1. Circuits for measuring projective-unitary invariants of a tuple of states. (a) SWAP test to measure the two-state overlap $\Delta_{12} = |\langle\psi_1|\psi_2\rangle|^2$. The probability of outcome 0 is $p(0) = (1+\Delta_{12})/2$. (b) Cycle test to measure the m-state invariant $\Delta_{12\cdots m}$. If the white square is the identity, we have $p(0) = (1+\Re(\Delta_{12\cdots m}))/2$. If the white square is the $P = \mathrm{diag}(1,i)$ gate, we have $p(0) = (1+\Im(\Delta_{12\cdots m}))/2$. The controlled gate implements the cyclic permutation $(123\cdots m)$ of the inputs if the control is in state $|1\rangle$, and does nothing otherwise.

Proof. We start with the connection between PU equivalence of two tuples of pure states $\Psi = (\psi_i)_{i=1}^N$, $\Phi = (\phi_i)_{i=1}^N$ and unitary equivalence between the associated tuples of wave-functions. Namely, Ψ is PU equivalent to Φ if and only if it is possible to find representing wave functions $\mathcal{A} = (|\psi_i\rangle)_{i=1}^N$, $\mathcal{B} = (|\phi_i\rangle)_{i=1}^N$ that are unitarily equivalent. That is, there exists an unitary operator U such that $|\phi_i\rangle = U|\psi_i\rangle$, for $i = 1,\ldots,N$. The problem of unitary equivalence of tuples of vectors is equivalent to equality of the corresponding Gram matrices i.e. $G_{ij}^{\mathcal{A}} = \langle\psi_i|\psi_j\rangle = \langle\phi_i|\phi_j\rangle = G_{ij}^{\mathcal{B}}$ (this follows e.g. from the uniqueness the Cholesky decomposition of G [27]). The phase of individual wave functions $|\psi_i\rangle$ is an unphysical, gauge degree of freedom, and therefore the Gram matrix of a collection of pure states Ψ is uniquely defined only up to conjugation via a diagonal unitary matrix. Assume now that for every tuple of quantum states $\Psi = (\psi_i)_{i=1}^N$ we have a construction (presented in the next paragraph) of a valid Gram matrix $\tilde{G}^{\Psi}$ whose entries can be expressed solely in terms of PU-invariants of states from Ψ. It then follows from the above considerations that Ψ is PU equivalent to Φ if and only if $\tilde{G}^{\Psi} = \tilde{G}^{\Phi}$.

The construction of $\tilde{G}^{\Psi}$ proceeds as follows. We first introduce the frame graph Γ^{Ψ} as an (undirected) graph whose vertices are labeled by $i = 1,\ldots,N$ with edges connecting i and j if and only if $\mathrm{tr}(\psi_i\psi_j) \neq 0$. Without loss of generality we assume that Γ^{Ψ} is connected [28] i.e. that every pair of vertices in Γ^{Ψ} can be connected via a path in Γ^{Ψ}. We can now choose a subgraph of Γ^{Ψ}, denoted by $\mathcal{T}^{\Psi}$, which is connected and contains the same vertices as Γ^{Ψ}, but no cycles. This is known as a *spanning tree* of Γ^{Ψ}, and there exists at least one spanning tree for any connected graph [29]—see figure 2 for an illustration. We now choose vector representatives $|\psi_i\rangle$ of states in Ψ in such a way that, for $\{i,j\}$ an edge in $\mathcal{T}^{\Psi}$, $\langle\psi_i|\psi_j\rangle = |\langle\psi_i|\psi_j\rangle|$. Every other inner product $\langle\psi_i|\psi_j\rangle$ will be either 0, or its phase will be fixed as follows. We first find a path from j to i within $\mathcal{T}^{\Psi}$. Since $\mathcal{T}^{\Psi}$ is a spanning tree, such a path is guaranteed to exist and to be unique. Suppose this path has k vertices $(\alpha_1 = j, \alpha_2, \ldots, \alpha_{k-1}, \alpha_k = i)$. Consider now the k-cycle that would be formed by adding the vertex j at the end of this path (note that vertices i and j are connected by an edge in Γ^{Ψ}) and denote it by C_{ij}. By construction, every edge in C_{ij} except for $\{i,j\}$ is in $\mathcal{T}^{\Psi}$, and therefore all the inner products $\langle\psi_{\alpha_l}|\psi_{\alpha_{l+1}}\rangle$ for $l \in \{1,2,\ldots k-1\}$ have been chosen as positive. Hence, if we denote the degree-k Bargmann invariant associated to C_{ij} as $\Delta(C_{ij}) := \Delta_{\alpha_1\alpha_2\ldots\alpha_{k-1}\alpha_k}$ we can write

$$\Delta\left(C_{ij}\right) = \langle\psi_i|\psi_j\rangle \prod_{l=1}^{k-1} \langle\psi_{\alpha_l}|\psi_{\alpha_{l+1}}\rangle\,. \tag{2}$$

Therefore, we can fix the phase of every nonzero inner product that is not in $\mathcal{T}^{\Psi}$ as $\langle\psi_i|\psi_j\rangle = \Delta(C_{ij})/\prod_{l=1}^{k-1}\langle\psi_{\alpha_l}|\psi_{\alpha_{l+1}}\rangle$. The above construction is reminiscent of the procedure of gauge fixing used in

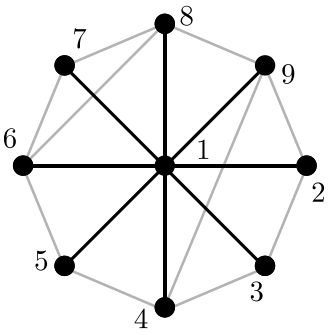

Figure 2. Frame graph for the example described in the text. Edges in black correspond to the choice of spanning tree, in this case a star graph.

the studies of magnetic fields and quantum statistics on graphs [30, 31]. Thus, all matrix elements of the so-constructed Gram matrix $\tilde{G}^{\Psi}_{ij} = \langle\psi_i|\psi_j\rangle$ are expressed via Bargmann invariants of degree at most N. The total number of invariants required to construct $\tilde{G}^{\Psi}$ in this way is upper-bounded by $(N-1)^2$, as we first measure $N(N-1)/2$ degree-2 invariants to obtain the frame graph, and then at most $(N-1)(N/2-1)$ additional invariants to fix the phases of the non-null elements of $\tilde{G}^{\Psi}$ corresponding to edges $\{i,j\} \notin \Gamma^{\Psi}$. □

Crucially, we cannot characterize the relational properties of even single-qubit states without using Bargmann invariants of degree $m > 2$. As an example, take two triples of single-qubit states $\Psi = (|X_+\rangle\langle X_+|, |Y_+\rangle\langle Y_+|, |Z_+\rangle\langle Z_+|)$, $\Phi = (|X_+\rangle\langle X_+|, |Y_-\rangle\langle Y_-|, |Z_+\rangle\langle Z_+|)$, where $|P_\pm\rangle\langle P_\pm|$ are projectors on Pauli eigenvectors with ± 1 eigenvalues. All overlaps within each tuple have the same value $\Delta_{ij} = 1/2$. Therefore, the tuples only differ in that $\Delta^{\Psi}_{123} = \frac{1+i}{4} \neq \frac{1-i}{4} = \Delta^{\Phi}_{123}$.

Let us now consider an application of theorem 1 to a $N = 9$ state tuple $(\psi_i)_{i=1\ldots 9}$. The first step is to construct the frame graph. This is done by measuring all $N(N-1)/2 = 36$ overlaps $\left|\langle\psi_i|\psi_j\rangle\right|$. Suppose the frame graph is the one represented in figure 2(recall that missing edges correspond to null overlaps). One choice of spanning tree is a star graph, where vertex 1 is connected to every other. We can fix the phases so that all inner products $\langle\psi_1|\psi_i\rangle > 0$. Finally, we consider all cycles that can be built by adding edges from the original frame graph to the spanning tree (in figure 2, these correspond to gray edges). In each such cycle, there is only one new edge whose phase has yet to be fixed; in this example only 3-cycles appear. We then measure the degree-3 Bargmann invariants Δ_{1ij} for all distinct pairs $\{i,j\}$, and attribute its phase to edge $\{i,j\}$. There are 28 of these for this example size, though in figure 2 only 10 of them are nonzero. This procedure leads to the Gram matrix:

$$\tilde{G}^{\Psi}_{ij} = \begin{cases} \sqrt{\Delta_{ii}} = |\langle\psi_i|\psi_i\rangle| = 1 & \text{for } i = j \\ \sqrt{\Delta_{1j}} = \left|\langle\psi_1|\psi_j\rangle\right|, & \text{for } i = 1, \\ \frac{\Delta_{ij1}}{\sqrt{|\Delta_{1j}||\Delta_{1i}|}} & \text{for } j > i. \end{cases} \tag{3}$$

The gauge choices involved in defining the Gram matrix $\tilde{G}^{\Psi}$ make all its entries measurable using the cycle test circuits, and capable of fully characterizing the relational information among states in Ψ.

The choice of spanning tree is not unique. In the above example, we could have chosen instead e.g. a simple path starting in vertex 1 and visiting all vertices sequentially up to vertex 9. Building the Gram matrix $\tilde{G}^{\Psi}$ using this path requires the same number of invariants, but they are more experimentally involved to measure, as some will have degree > 3. An interesting open question is to find alternative characterization procedures for general scenarios that minimize the experimental effort required.

2.3. Robustness, sample complexity, and mixed states

Any implementation of cycle tests will have to deal with experimental imperfections and, at at best, mixed-state approximations of the ideal pure states. In [32] we give an argument that, as long as the prepared density matrices have high purity, then the Bargmann invariants measured will be close to the Bargmann invariants of the target pure states (understood to be the projector onto the eigenvector corresponding to the largest eigenvalue of a density matrix). In [32] we also show that if Bargmann invariants evaluated for two tuples of pure states $\Psi = (\psi_i)_{i=1}^N$, $\Phi = (\phi_i)_{i=1}^N$ differ from each other only slightly, then states comprising them can be *approximately transformed onto each other*. Specifically, we show that there exists a unitary

transformation U that *approximately* transforms Ψ onto Φ in the sense that (under mild assumptions specified in [32])

$$\frac{1}{N}\sum_{i=1}^{N}\left(1-\mathrm{Tr}\left(U\psi_i U^\dagger \phi_i\right)\right) \leqslant \frac{C_\Psi}{N}\|\tilde{G}^\Psi - \tilde{G}^\Phi\|_2^2\,, \tag{4}$$

where C_Ψ is a constant (depending on Ψ), $\tilde{G}^\Psi, \tilde{G}^\Phi$ are Gram matrices from the proof of Theorem 1, and $\|X\|_2 = \sqrt{\mathrm{Tr}(X^2)}$ is the Hilbert–Schmidt norm. This shows that Bargmann invariants offer a robust characterization of relational properties of tuples of pure states. Inequality (4) also serves to analyse the expected estimation errors due to a finite number of cycle test runs. Specifically, from Hoeffding's inequality it follows that estimation of a single Bargmann invariant to accuracy ϵ with probability greater than $1-\delta$ requires $\Theta(1/\epsilon^2)\log(1/\delta)$ experimental cycle test shots. It follows that $s_{\mathrm{rel}} = \Theta(N^2\log(N/\delta)/\epsilon^2)$ experiments suffice to estimate all necessary Bargmann invariants up to accuracy ϵ with high probability. For comparison, the sampling cost of standard tomographic reconstruction of N pure states up to accuracy ϵ in trace norm equals $s_{\mathrm{tom}} = \Theta(Nd\log(N/\delta)/\epsilon^2))$ [33]. Our procedure is much more economical, as the sampling complexity depends solely on number of states N, and not on the dimension d of the Hilbert space—in principle our scheme, contrary to usual tomography, can be realized even in infinite-dimensional spaces. Furthermore, under reasonable assumptions estimation of all necessary Bargmann invariants up to accuracy ϵ allows to approximately characterize relational information in Ψ [34].

Identifying complete sets of PU-invariants for mixed states is a much more challenging problem. If we use mixed states ρ_i $(i = 1, 2, \ldots, m)$ as inputs to the cycle test circuits of figure 1, the output gives an operational meaning to mixed-state Bargmann invariants: $\Delta_{12\ldots m} = \mathrm{Tr}\left(\rho_1\rho_2\ldots\rho_m\right)$. Mixed-state invariants of this form are also known as multivariate traces [15], with proposed applications in quantum error mitigation [17]. In [32] we show that for a tuple of N mixed states $\mathcal{S} = (\rho_i)_{i=1}^N$ in dimension d, Bargmann invariants of degree $m \leqslant d^2$ form a complete set of invariants characterizing PU invariant properties of $\mathcal{S}$. Moreover, the number of independent invariants can be chosen to be Nd^2+1. These results follow from known results from invariant theory [16, 35, 36], which we (partially) reprove with the help of Schur–Weyl duality.

2.4. Applications

Testing for linear independence. Whether a set of states is linearly independent (LI) is clearly a unitary-invariant property. LI states can be probabilistically cloned, and can be unambiguously discriminated. Recognizing linear dependence of a set of states enables us to find a more compact description of the set; in machine learning, this corresponds to a procedure for dimensionality reduction. Using a complete set of Bargmann invariants, we can compute the hypervolume generated by the set of states to determine whether they are LI. For the case of m non-orthogonal vectors, we can use the Gram matrix encoding of the complete set of invariants we have described to write the linear independence condition simply as: $\det(G) > 0$. In [32] we calculate $\det(G)$ explicitly as a function of the invariants for the cases of 3 and 4 non-orthogonal states.

Basis-independent imaginarity witnesses. Measuring Bargmann invariants of degree 3 and above can serve as a basis-independent witness that the input quantum states have complex-valued amplitudes. The simple reason is that if $\Im(\Delta_{12\ldots m}) \neq 0$ some of the density matrices at the input must necessarily have complex-valued entries, independently of the basis chosen. As an example, it is easy to check that the 3 Pauli operator eigenstates $|A\rangle = |0\rangle, |B\rangle = \frac{1}{\sqrt{2}}(|0\rangle + |1\rangle), |C\rangle = \frac{1}{\sqrt{2}}(|0\rangle + i|1\rangle)$ achieves the maximum value of $\Im(\Delta_{ABC}) = 1/4$ for this 3-state scenario. In [32] we describe a tuple of n single-qubit states that are vertices of a regular spherical n-gon on the Bloch sphere, for which $\Im(\Delta) \to 1$ as $n \to \infty$.

Experimental tests have been recently proposed to discriminate whether complex amplitudes (or 'imaginarity') are an essential feature of quantum theory [37, 38]. The application of our proposal as an imaginarity witness differs from that of [37] in that it is not device-independent, despite being basis-independent.

Basis-independent coherence witnesses. If the m states ρ_i are simultaneously diagonalizable in a single reference basis, the degree-m Bargmann invariant $\Delta_{12\ldots m} = \mathrm{Tr}(\prod_i \rho_i)$ is simply the probability that independent measurements of the reference basis on all states give the same outcome [39]. Hence, for diagonal states these invariants must be real and in the range $\Delta_{12\cdots m} \in [0, 1]$. Measuring $\Im(\Delta_{12\ldots m}) \neq 0$, or real values outside of the allowed range for diagonal states, serves as a basis-independent witness of coherence, generalizing the overlap-based witnesses of [39]; an alternative approach to quantify basis-independent coherence has been recently proposed in [40]. Note that witnesses of imaginarity, as discussed in the previous section, are also witnesses of coherence, as complex-valued entries of a density matrix must be off-diagonal. In [32] we look at the simplest scenarios where coherence can be witnessed by Bargmann invariant measurements when we have sets with either 2 or 3 states.

Characterization of photonic indistinguishability. Bargmann invariants have helped describe experiments using single photons in linear optics [8]. Each photon in an m-photon experiment is described by a state over its internal degrees of freedom—such as polarization and orbital angular momentum [41]. Suppose we apply some linear-optical transformation to these photons that is insensitive to their internal degrees of freedom, and measure output occupation numbers. The outcome statistics will not depend on exactly which internal state a particular photons is in, but it will depend on the relational information, such as imperfect overlaps, which bring about partial distinguishability. In other words, the output probabilities of such an experiment can only depend on the linear-optical transformation and on the Bargmann invariants of the set of states. This can be seen in several recent experimental and theoretical works concerning genuine 3- and 4-photon indistinguishability [5–7, 39, 42].

In [39], it was shown how measurements of some overlaps among a set of m states can result in nontrivial lower bounds for all overlaps. Bargmann invariants of higher degree can be useful in the same way, as by definition $|\Delta_{12\ldots m}|^2$ is a lower bound to overlaps of all neighboring states in the associated cycle. This suggests improved designs for photonic measurements of Bargmann invariants may help in the characterization of multi-photon sources.

3. Discussion

We reviewed how Bargmann invariants encode the projective-unitary invariant properties of a set of states. For the case of pure states, we have shown how to represent the complete information in a Gram matrix of inner products, written in terms of invariant quantities only, representing relational information about the states in the set. We have proposed a way of measuring real and imaginary parts of arbitrary Bargmann invariants using cycle tests, a natural generalization of the SWAP test. We discussed several applications: coherence and imaginarity witnesses, testing for linear independence, and characterization of multi-photon indistinguishability. Open problems include finding efficient NISQ methods for measuring and using Bargmann invariants in algorithmic applications, studying possible applications to self-testing in a semi-device independent context [43, 44], and developing further the resource theories of imaginarity and coherence based on Bargmann invariants, whose first steps we have described.

4. Methods

4.1. Efficient constructions for cycle test circuits

The main ingredient of the cycle test is a controlled permutation gate which applies a cyclic permutation when the control qubit is in the $|1\rangle$ state (and does nothing otherwise). We now describe two efficient ways of implementing this controlled cycle permutation. For simplicity, we consider first how to decompose a cyclic permutation in terms of pairwise permutations (i.e. transpositions), without accounting for the control qubit, to which we return at the end of this section.

Let us denote $C_k = (1,2,3,\ldots,k)$ as the cyclic permutation on k elements, and (i,k) as a permutation of two elements (or transposition) i and k. A well-known decomposition of a cyclic permutation in terms of transpositions is given by

$$(1,2,3,\ldots,k) = (1,2)\,(2,3)\ldots(k-1,k)\,. \tag{5}$$

This decomposition uses only adjacent transpositions, which is equivalent to swapping only nearest-neighbor qubits at a time. It leads to a circuit as exemplified in figure 3. This circuit uses the optimal number of $(k-1)$ nearest-neighbor transpositions and has depth $(k-1)$. That $(k-1)$ is the optimal number follows from the need to move the first element to the last position, which requires exactly $(k-1)$ nearest-neighbor transpositions.

It is possible to give an alternative decomposition that has much smaller depth, at the cost of using longer-range transpositions. To see it, consider first the following Lemma:

Lemma 1. *Consider the following two disjoint cycles* $(1,2,\ldots k)$ *and* $(k+1,k+2,\ldots,n)$*. We have the following decomposition:*

$$C_n\,(1,\ldots,n) = (1,k+1)\,(1,2,\ldots k)\,(k+1,k+2,\ldots,n)\,. \tag{6}$$

The proof of this Lemma is straightforward, it simply requires checking the images of numbers $1, k, k+1$, and n under the sequence of permutations, as all other numbers get trivially mapped to the correct places.

A very efficient decomposition of C_m can now be obtained by applying lemma 1 repeatedly. Suppose, for simplicity, that m is a power of 2. Then we can first decompose C_m into two cycles acting on $m/2$ elements

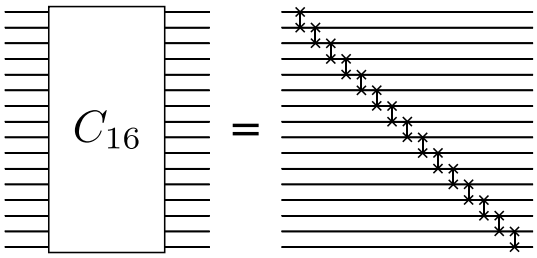

Figure 3. Decomposition of a 16-qubit cyclic permutation in terms of nearest-neighbor SWAP gates.

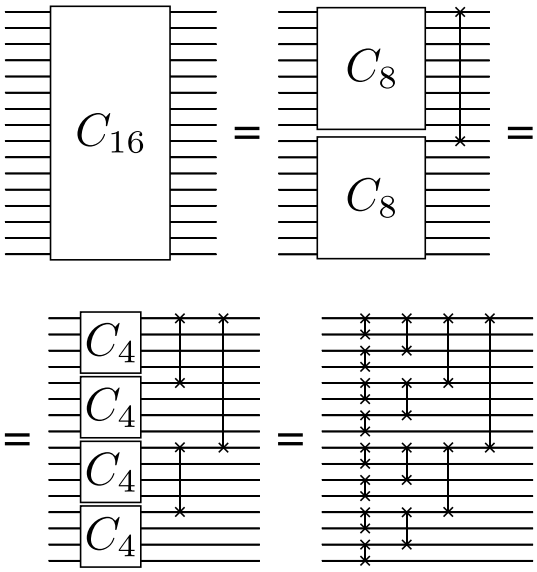

Figure 4. Decomposition of a 16-qubit cyclic permutation in terms of SWAP gates. This circuit is much more parallelized compared to that of figure 3, although the trade-off is the requirement of long-range swaps.

followed by one transposition, i.e. $C_m = (1, m/2+1)(1,2,\ldots,m/2)(m/2+1, m/2+2\ldots m)$. We then break each cycle of size $m/2$ again in two cycles, acting each on $m/4$ elements. This divide-and-conquer algorithm is iterated until all that is left are transpositions. It is easy to see that this procedure terminates after $\mathrm{O}(\log m)$ steps, and hence that the final circuit has depth $\mathrm{O}(\log m)$ as well. An example of this for $m = 16$ is shown in figure 4.

These are not the only decompositions of the cycle permutation in terms of transpositions, but they represent two extreme regimes. In the first, we have only nearest-neighbor SWAP gates, but the depth of the circuit is large. In the second, the depth is logarithmic, but longer-range gates are required. Which is the most efficient depends on the constraints of the particular architecture being used—the latter has the benefit of mitigating accumulation of errors in the circuit, but in particular architectures long-range gates might not be an option.

Let us now return to the issue of decomposing a *controlled* cycle permutation. At first glance, neither decomposition we described has the promised properties. The circuit in figure 3 is no longer composed only of nearest-neighboring controlled-SWAP (or Fredkin) gates, since the first qubit must control the swapping of states that are distant to it. At the same time, the circuit of figure 4 does not have logarithmic depth since every gate in the circuit must be controlled by the same control qubit, which presumably means that all gates must be done sequentially. Nonetheless, both circuits can be adapted to restore the desired properties, as follows.

In figure 5 we show how the controlled version of circuit in figure 3 can be implemented using only gates (SWAP and Fredkin) that act on neighboring qubits.

To obtain a controlled version of figure 4 that has depth $\mathrm{O}(\log m)$, as in the original, we need to include more ancilla qubits to parallelize the control operation. Instead of controlling the permutations with a single $\frac{1}{\sqrt{2}}(|0\rangle + |1\rangle)$, we need to build an $m/2$-qubit GHZ state $\frac{1}{\sqrt{2}}(|0\rangle^{\otimes m/2} + |1\rangle^{\otimes m/2})$, such that each qubit in this

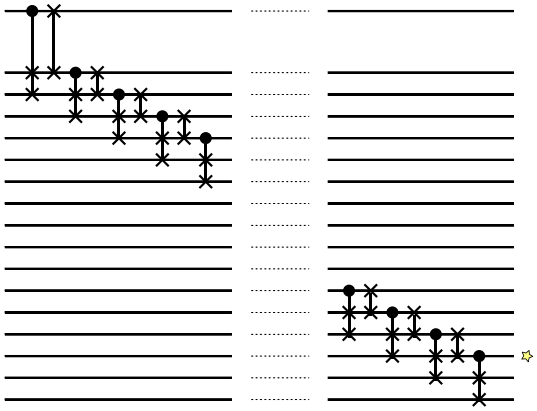

Figure 5. An adaptation of the circuit of figure 3 that obtains a controlled cycle permutation with SWAP and Fredkin gates acting only on neighboring state. The first qubit is swapped along the 1D chain as each Fredkin gate is applied. The star at the output indicates where the control qubit is effectively left at the end of the circuit.

state can control a different SWAP gate in parallel. The whole construction still has logarithmic depth due to the follow Lemma (also cf figure 2 in [45]):

Lemma 2 ([45]). *The m-qubit GHZ state:*

$$\frac{1}{\sqrt{2}}\left(|0\rangle^{\otimes m}+|1\rangle^{\otimes m}\right) \tag{7}$$

can be generated by a circuit that acts on the $|0\rangle^{\otimes m}$ *state, is composed only of a single Hadamard and a sequence of CNOT gates, and has depth* $O(\log m)$.

Proof. We initialize m qubits in the $|0\rangle^{\otimes m}$ state, and apply a Hadamard gate to the first one. Our goal is now to apply a sequence of CNOT gates that will flip every qubit conditioned on the first qubit being $|1\rangle$ and does nothing otherwise. This can be done as follows. In the first round, we apply a CNOT gate from qubit 1 to qubit 2. In the second round, we apply two CNOTs, from qubits 1 and 2 to qubits 3 and 4, respectively. We repeat this procedure by reusing previously flipped qubits as controls for the next layer. The number of qubits flipped in this manner doubles with each layer. Hence, it follows that this will generate an m-qubit GHZ state in $O(\log m)$ layers of two-qubit gates. □

For the controlled version of figure 4 to work properly when using the GHZ state as the ancilla, we need to perform the operation described in the proof of lemma 2 in reverse at the end of the cycle test protocol. This is required to disentangle the ancillas with the control qubit, such that interference can occur properly at the last H gate in figure 1 (in the main text). In any case, it follows that the entire controlled-cycle protocol works in depth $O(\log m)$.

Very recently, independent work has proposed cycle test circuits with constant depth [15], and circuits which allow trade-offs between number of auxiliary qubits and depth [17].

Data availability statements

The authors declare that the data supporting the findings of this study are available within the paper and in the Supplementary Information files.

No new data were created or analysed in this study.

Acknowledgments

We thank Adam Sawicki for his comments regarding the role of Schur-Weyl duality for the problem of PU equivalence of mixed states. M O acknowledges support by the Foundation for Polish Science through the TEAM-NET project (Contract No. POIR.04.04.00-00-17C1/18-00). D J B acknowledges support from Instituto Nacional de Ciência e Tecnologia de Informação Quântica (INCT-IQ, CNPq) and FAPERJ. E F G acknowledges funding of the Portuguese institution FCT—Fundação para Ciência e Tecnologia via Project CEECINST/00062/2018. This work was supported by the H2020-FETOPEN Grant PHOQUSING (GA No. 899544).

Author contribution

M O, D J B, E F G conceived the main idea, and developed the theory jointly. E F G proposed a simple version of the cycle circuits, whose design was improved on by D J B. M O contributed with theorem proofs on robustness and the mixed-state case. All authors contributed to discussing the results, proposing applications, and writing the paper.

Conflict of interests

The authors declare no competing financial or non-financial interests.

ORCID iD

Daniel J Brod https://orcid.org/0000-0002-5925-4158

References

[1] Klein F 1900 *Bull. New York Math. Soc.* **2** 215
[2] Leifer M S, Linden N and Winter A 2004 *Phys. Rev.* A **69** 052304
[3] Bargmann V 1964 *J. Math. Phys.* **5** 862
[4] Chien T-Y and Waldron S 2016 *SIAM J. Discrete Math.* **30** 976
[5] Menssen A J, Jones A E, Metcalf B J, Tichy M C, Barz S, Kolthammer W S and Walmsley I A 2017 *Phys. Rev. Lett.* **118** 153603
[6] Jones A E, Menssen A J, Chrzanowski H M, Wolterink T A W, Shchesnovich V S and Walmsley I A 2020 *Phys. Rev. Lett.* **125** 123603
[7] Minke A M, Buchleitner A and Dittel C 2021 *New J. Phys.* **23** 073028
[8] Simon R and Mukunda N 1993 *Phys. Rev. Lett.* **70** 880
[9] Dariusz Chruscinski A J 2004 *Geometric Phases in Classical and Quantum Mechanics* (*Progress in Mathematical Physics*) 1st edn (Birkhäuser Boston)
[10] Kirkwood J G 1933 *Phys. Rev.* **44** 31
[11] Dirac P A M 1945 *Rev. Mod. Phys.* **17** 195
[12] Bamber C and Lundeen J S 2014 *Phys. Rev. Lett.* **112** 070405
[13] Pancharatnam S 1956 *Proc. Indian Acad. Sci.* A **44** 247
[14] Samuel J and Bhandari R 1988 *Phys. Rev. Lett.* **60** 2339
[15] Qwek Y, Kaur E and Wilde M M 2022 arXiv:2206.15405 [quant-ph]
[16] Wigderson A 2019 *Mathematics and Computation: A Theory Revolutionizing Technology and Science* (Princeton University Press)
[17] Liang J-M, Lv Q-Q, Wang Z-Xi and Fei S-M 2023 *Phys. Rev.* A **107** 012606
[18] Reascos L I, Murta B, Galvão E F and Fernández-Rossier J 2023 *Phys. Rev. Res.* **5** 043087
[19] Wagner R and Galvão E F 2023 *Phys. Rev.* A **108** L040202
[20] Wagner R, Schwartzman-Nowik Z, Paiva I L, Te'eni A, Ruiz-Molero A, Barbosa R S, Cohen E and Galvão E F arXiv:2302.00705 [quant-ph]
[21] Barenco A, Berthiaume A, Deutsch D, Ekert A, Jozsa R and Macchiavello C 1997 *SIAM J. Comput.* **26** 1541
[22] Buhrman H, Cleve R, Watrous J and de Wolf R 2001 *Phys. Rev. Lett.* **87** 167902
[23] Ekert A K, Alves C M, Oi D K L, Horodecki M, Horodecki P and Kwek L C 2002 *Phys. Rev. Lett.* **88** 217901
[24] Knill E and Laflamme R 1998 *Phys. Rev. Lett.* **81** 5672
[25] Aharonov D, Jones V and Landau Z 2009 *Algorithmica* **55** 395–421
[26] Chefles A, Jozsa R and Winter A 2004 *Int. J. Quant. Inf.* **2** 11–21
[27] Johnston N 2021 *Advanced Linear and Matrix Algebra* (Springer)
[28] If G^{Ψ} is not connected then the problem of PU equivalence of states from Ψ reduces to independent problems concerning states associated with connected components in Γ^{Ψ}
[29] Gross J and Yellen J 1998 *Graph Theory and Its Applications, Second Edition* (*Discrete Mathematics and Its Applications*) (Taylor & Francis)
[30] Harrison J M, Keating J P and Robbins J M 2011 *Proc. R. Soc.* A **467** 212
[31] Harrison J M, Keating J P, Robbins J M and Sawicki A 2014 *Commun. Math. Phys.* **330** 1293
[32] Supplemental material, which includes [45–50]
[33] Haah J, Harrow A W, Ji Z, Wu X and Yu N 2017 Sample-optimal tomography of quantum states *IEEE Trans. Inf. Theory* **63** 5628
[34] Let us assume that: a) the frame Graph Γ^{Ψ} is known and b) the overlaps between pure states $G^{\Psi}_{ij} = \mathrm{tr}(\psi_i\psi_j)$ are known up to relative precision Δ (these can be obtained from $\Theta(N^2\log(N/\delta)/(\min_{ij}|G_{ij}|\Delta^2))$ shots). Then, the estimation of the remaining necessary invariants requires $s_{rel} = \Theta(N^2\log(N/\delta)/\epsilon^2)$ experimental shots. Results of these experiments provide estimate for the Gram matrix $\tilde{G}^{\Psi}_{est}$ such that $\|\tilde{G}^{\Psi}_{est} - \tilde{G}^{\Psi}\|_{\mathrm{HS}}$ can be easily bounded as a function of ϵ and the magnitude of the smallest entry of $\tilde{G}^{\Psi}$: $G^{\Psi}_{\min} = \min|\mathrm{tr}(\psi_i\psi_j)|$. Specifically, it can be shown that by choosing, for a fixed Ψ, the accuracy parameter $\epsilon = 1/\mathrm{poly(N)}$ the distance $\|\tilde{G}^{\Psi}_{est} - \tilde{G}^{\Psi}\|_{\mathrm{HS}}$ is bounded by a polynomially decaying function of N.
[35] Procesi C 1976 *Adv. Math.* **19** 306
[36] Formanek E 1991 *The Polynomial Identities and Invariants of N X N Matrices* (*Cbms Regional Conference Series*) (Conference Board of the Mathematical Sciences)
[37] Renou M-O, Trillo D, Weilenmann M, Thinh L P, Tavakoli A, Gisin N, Acin A and Navascues M 2021 (arXiv:2101.10873 [quant-ph])
[38] Wu K-D, Kondra T V, Rana S, Scandolo C M, Xiang G-Y, Li C-F, Guo G-C and Streltsov A 2021 *Phys. Rev. Lett.* **126** 090401
[39] Galvão E F and Brod D J 2020 *Phys. Rev.* A **101** 062110
[40] Designolle S, Uola R, Luoma K and Brunner N 2021 *Phys. Rev. Lett.* **126** 220404
[41] Tichy M C 2015 *Phys. Rev.* A **91** 022316
[42] Giordani T, Esposito C, Hoch F, Carvacho G, Brod D J, Galvão E F, Spagnolo N and Sciarrino F 2021 *Phys. Rev. Res.* **3** 023031

[43] Tavakoli A, Kaniewski J, Vértesi T, Rosset D and Brunner N 2018 *Phys. Rev.* A **98** 062307
[44] Miklin N and Oszmaniec M 2021 *Quantum* **5** 424
[45] Cruz D *et al* 2019 *Adv. Quantum Technol.* **2** 1900015
[46] Arias-Castro E, Javanmard A and Pelletier B 2020 *J. Mach. Learn. Res.* **21** 498–534
[47] Fulton W and Harris J 1991 *Representation Theory: A First Course* (*Graduate Texts in Mathematics*) (Springer)
[48] Goodman R and Wallach N 2009 *Symmetry, Representations and Invariants* (*Graduate Texts in Mathematics*) (Springer)
[49] Vrana P 2012 *PhD Thesis* (available at: https://s3.cern.ch/inspire-prod-files-e/ed42c58dae972ae848cdaa887b1c9ce9)
[50] Bergou J A, Futschik U and Feldman E 2012 *Phys. Rev. Lett.* **108** 250502